

# CHAPTER 3

## DARK CURRENT AND NOISE

### **3.1 Dark current**

- 3.1.1 Leakage currents
- 3.1.2 Thermionic emission
- 3.1.3 Field emission
- 3.1.4 Background radiation
- 3.1.5 Exposure
- 3.1.6 High-voltage polarity

### **3.2 Statistical nature of noise**

- 3.2.1 Photon noise
- 3.2.2 Cathode current fluctuations
- 3.2.3 Noise spectrum
- 3.2.4 Noise in scintillation detectors
- 3.2.5 Noise contribution of the electron multiplier
- 3.2.6 Johnson noise
- 3.2.7 Scintillation detection

### **3.3 Equivalent noise input and minimum discernible signal**

- 3.3.1 Definitions
- 3.3.2 Minimum value of noise equivalent power
- 3.3.3 Effect of bandwidth
- 3.3.4 Measurement of noise equivalent power

### **Appendix Noise statistics and bandwidth**

- A3.1 Practical scintillation spectra
- A3.2 Noise equivalent bandwidth

## **DARK CURRENT AND NOISE**

This chapter discusses disturbances that interfere with the current or voltage to be measured and limits the accuracy of the measurement. This includes principally dark current and noise.

### **3.1 Dark current**

The dark current is not, strictly speaking, a noise; however, noise that is associated with it does impose a limitation on the detection of very low energy radiation.

The current that flows in the anode circuit when voltage is applied to a photomultiplier in total darkness has two components:

- a continuous one due to leakage on glass and insulation surfaces,
- an intermittent one, consisting of pulses of a few nanoseconds duration.

The effect of the various causes of dark current varies according to the operating and environmental conditions (applied voltage, gain, temperature, humidity etc.), and also according to the tube's history (past storage and illumination conditions, etc.). Some of the causes are merely temporary in their effect, in which case the dark current eventually settles down to a stable level. Others are permanent.

The permanent causes of dark current (i.e. those that are independent of the history of the tube) are mainly:

- leakage currents
- thermionic emission
- field emission
- background radiation.

#### **3.1.1 Leakage currents**

These are the sole cause of the continuous component of the dark current and are due to the surface conductivity of the electrode supports, envelope, base, and socket. Surface conductivity on the inside of the tube is affected by the alkali metals used, and on the outside by agents such as dust, moisture and grease.

The dark current component due to leakage currents varies roughly linearly with the high voltage applied (that is, much less markedly than the gain, which varies exponentially at a high power of the voltage). It is therefore the predominant component when the tube operates at low gain. It is also the predominant component at low temperatures, where thermionic emission is less significant.

### 3.1.2 Thermionic emission

One of the main causes of the pulse component of the dark current is *thermionic emission* from the photocathode. This emission obeys Richardson's law

$$J = AT^2 \exp(-W_{th}/kT) \quad (3.1)$$

in which  $J$  represents current density,  $A$  is a constant,  $T$  is absolute temperature, and  $k$  is the Boltzmann constant. The term  $W_{th}$  is the thermionic work function of the photocathode material; for semiconductors, it is less than the photoemission threshold (§A1.1.3), being about 1 to 2 eV for cathodes sensitive to visible light.

Although the thermionic work function and the photoemission threshold are separate quantities, within a given family of tubes, there appears to be a statistical correlation that makes high red and infrared sensitivity incompatible with low dark current.

At room temperature, the thermionic emission of photocathodes with maximum sensitivity in the range 300 to 500 nm is between 10 and 1000 electrons/cm<sup>2</sup>s. It increases, however, as the sensitivity extends towards the long wavelengths (lower electron affinity) and with an S1(C) photocathode can be as high as a few million electrons/cm<sup>2</sup>s. Thermionic emission also occurs at the dynodes of the multiplier.

As Eq.3.1 shows, thermionic emission decreases rapidly as temperature decreases. Figure 3.1 shows the variation in the number of dark current pulses per second as a function of temperature for bialkline (SbKCs) cathodes and trialkaline cathodes with extended red sensitivity (SbNa<sub>2</sub>KCs). At normal temperatures, thermionic emission is the predominating cause of the dark current, at least at normal supply voltages. At low temperatures, it becomes negligible compared with other causes, and the dark pulse rate tends towards a plateau as the temperature decreases.

Dark pulses due to thermionic emission are mainly of the single-electron type (§2.3), and those originating in the electron multiplier are amplified less than those from the cathode. The amplitude distribution of the pulses depends largely on the multiplier design (Fig.2.9).

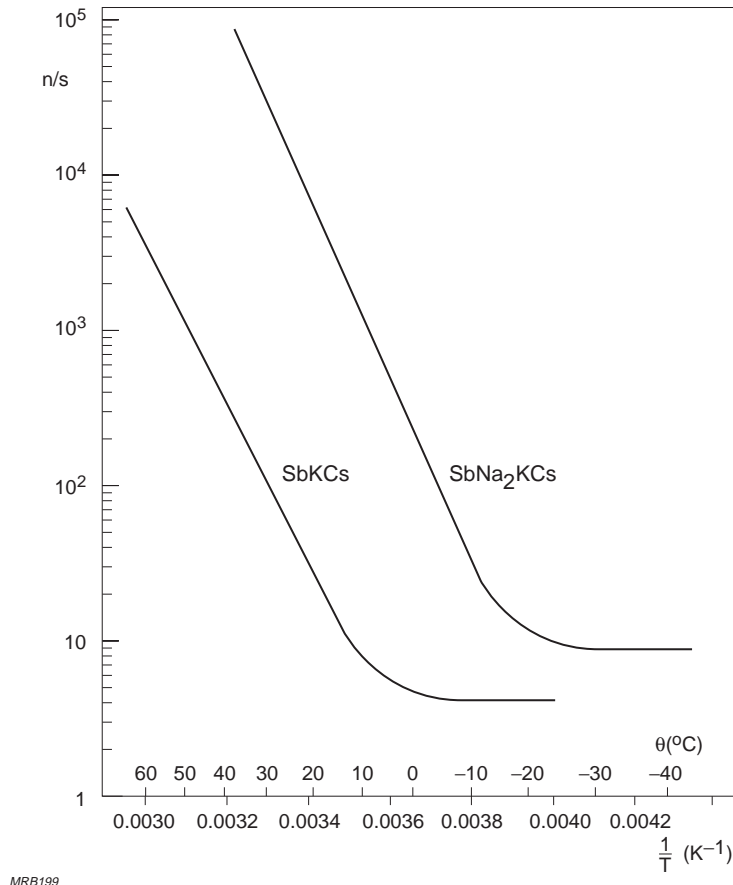


Fig.3.1 Number of dark pulses per second as a function of temperature, for SbKCs and SbNa<sub>2</sub>KCs photocathodes

### 3.1.3 Field emission

Although the electric fields in a photomultiplier are fairly low, there is some electron emission due to field effect (cold emission) because of inevitable roughness of the electrodes; this is aggravated by the adsorption of alkali metals (mainly caesium) at the electrode surfaces, which considerably reduces their electron affinity. Electrons emitted by field effect bombard the envelope glass and other surfaces causing emission of photons which can reach the photocathode.

The dark pulse rate due to field emission does not depend much on temperature. It does depend on the applied voltage, however, and increases faster than the gain, which is one of the principal factors that sets a practical limit to gain. Figure 3.2 shows the three ranges of supply voltage in which each of the three causes of dark current, so far discussed, predominates.

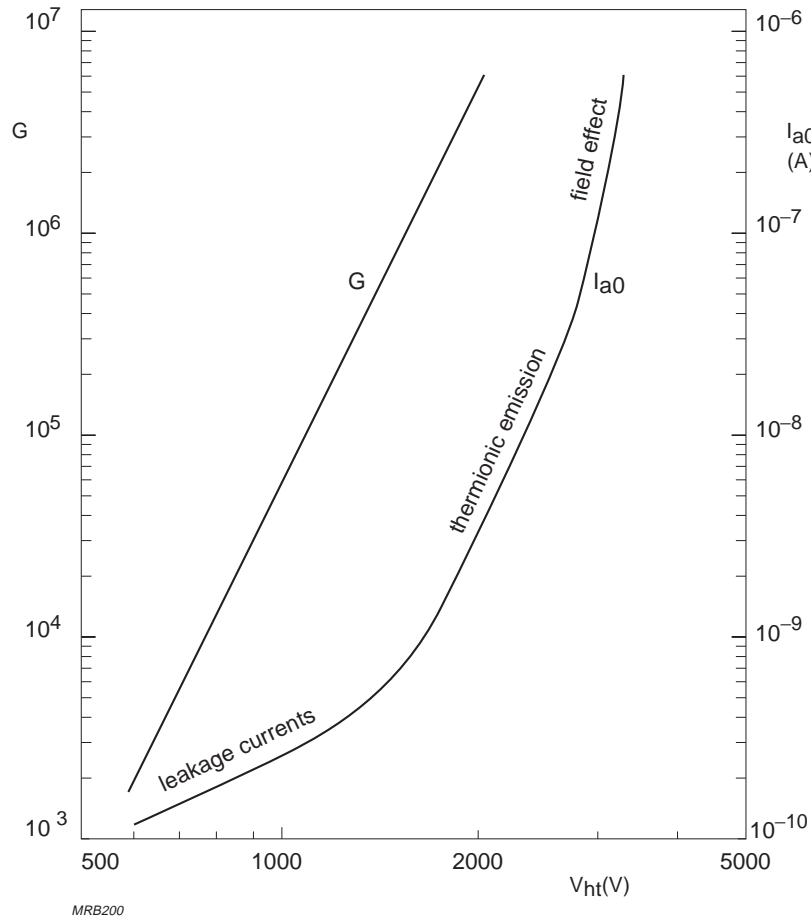


Fig.3.2 Major causes of dark current versus supply voltage

### 3.1.4 Background radiation

Background radiation, including that due to the materials of the tube (e.g.  $^{40}\text{K}$ ), is another cause of dark pulses. High energy charged particles (e.g. cosmic rays) can give rise to Cherenkov radiation in the tube window, which in turn causes photoemission. Cherenkov radiation can generate several photons at a time, so the dark pulses it causes (multi-electron noise) are often of high amplitude.

### 3.1.5 Exposure

Of the many *temporary* causes of dark current, the two most often encountered are previous exposure to light and negative-polarity connection of the photocathode.

Exposure to normal light, even when no voltage is applied, considerably increases the subsequent dark current, owing to excitation of the photocathode itself and the glass of the envelope. The dark current increase depends on the wavelength, the incident flux, and the duration of exposure. Figures 3.3 to 3.5 show how the dark current of an S13 photocathode ( $\text{SbCs}_3$  on fused silica) stabilizes after different conditions of exposure. (In the graphs, the number of electrons per second constituting the dark current during the stabilization period has been normalized with respect to the steady-state dark current.) After prolonged exposure to sunlight, the time required to stabilize the dark current may be as long as 48 hours. Hence the necessity of guarding photomultipliers against exposure to ambient light and, if possible, storing them in the dark when they are not in use.

A similar increase of dark current occurs if a photomultiplier in operation is accidentally subjected to a brief, intense flash of 'UV' light.

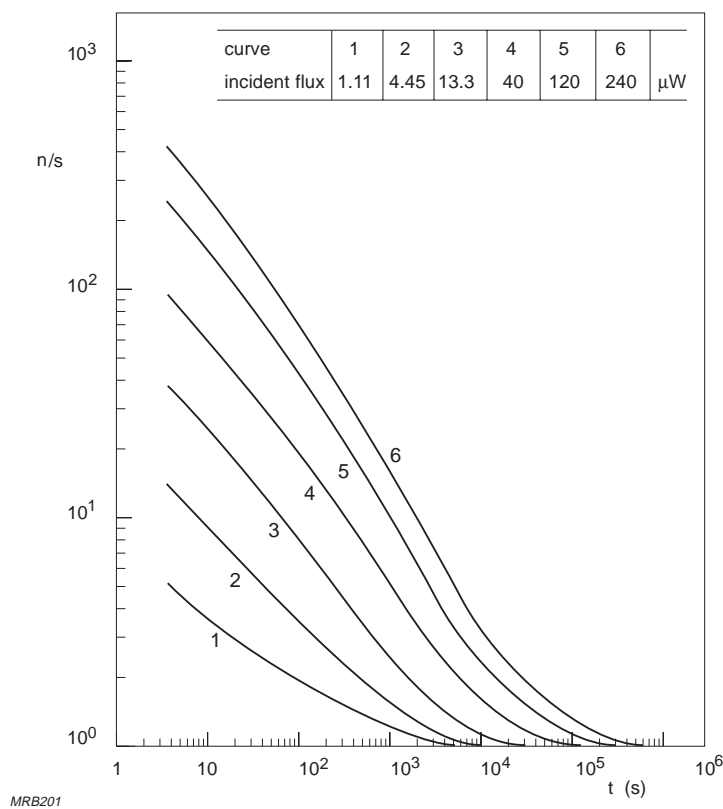


Fig.3.3 Dark-current decay of an S13 cathode at 0 °C following exposure for 100 s at  $\lambda = 366$  nm, with incident flux as parameter. Vertical scale, relative number of electrons per second

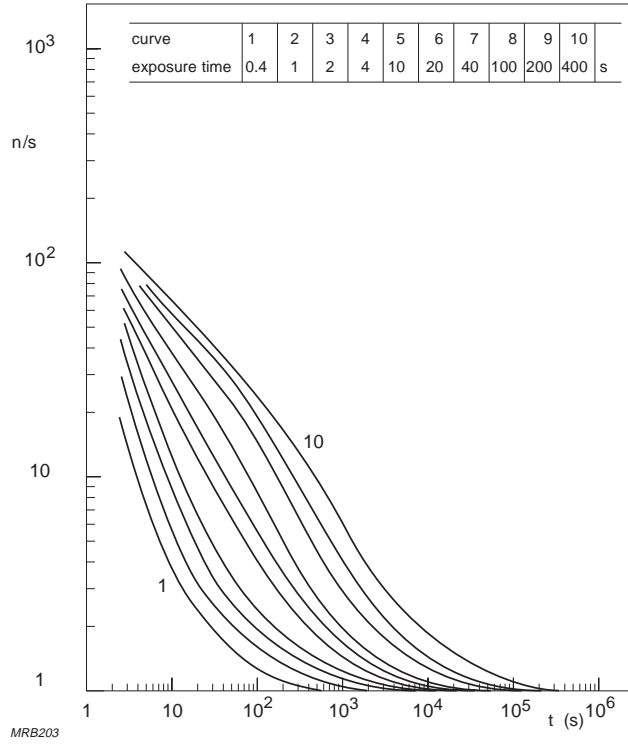


Fig.3.4 Dark-current decay of an S13 cathode at 0 °C following exposure to an incident flux of 120  $\mu\text{W}$  at  $\lambda = 366 \text{ nm}$ , with exposure time as parameter. Vertical scale, relative number of electrons per second

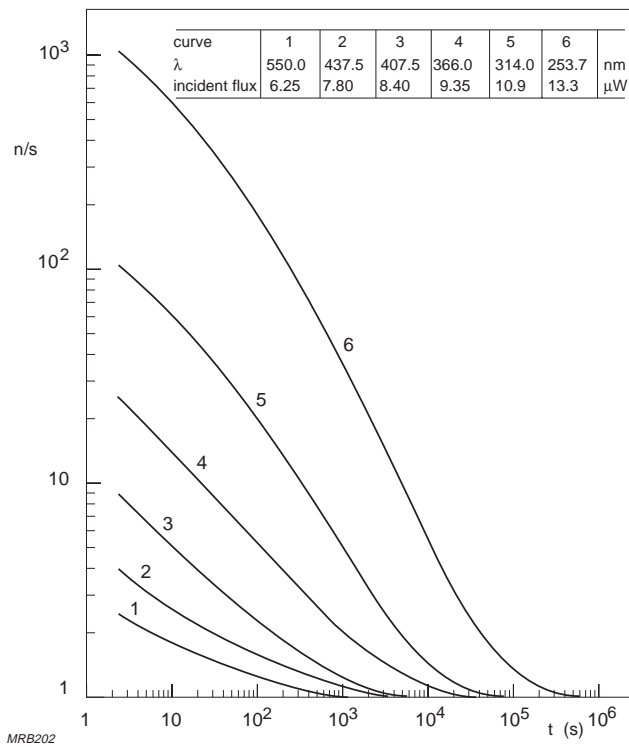


Fig.3.5 Dark-current decay of an S13 cathode at 0 °C following exposure for 100 s to equal numbers of photons, with wavelength as parameter ( $\phi \propto 1/\lambda$ ). Vertical scale, relative number of electrons per second

### 3.1.6 High-voltage polarity

In some applications it is necessary to ground the anode and apply a high negative potential to the cathode (§5.1). When this is done the dark current immediately assumes a value much higher than normal (curve 1, Fig.3.6) and may take more than half an hour to settle back. The lower the normal dark current is, the more pronounced the rise and the longer the settling time.

If a tube connected in negative polarity is not properly insulated from its surroundings, insulation breakdown may occur between the envelope and earth; this generates a high, unstable, dark current and can quickly destroy the tube by electrolysis of the glass. The risk can be guarded against by coating the wall of the tube with conductive paint, taken to photocathode potential through a protective resistor of about 10 M $\Omega$ , and/or enclosing it in an adequate thickness of insulation (§5.1).

When the photocathode is grounded and the anode positive, the dark current stabilizes quickly. This polarity should therefore be used whenever possible.

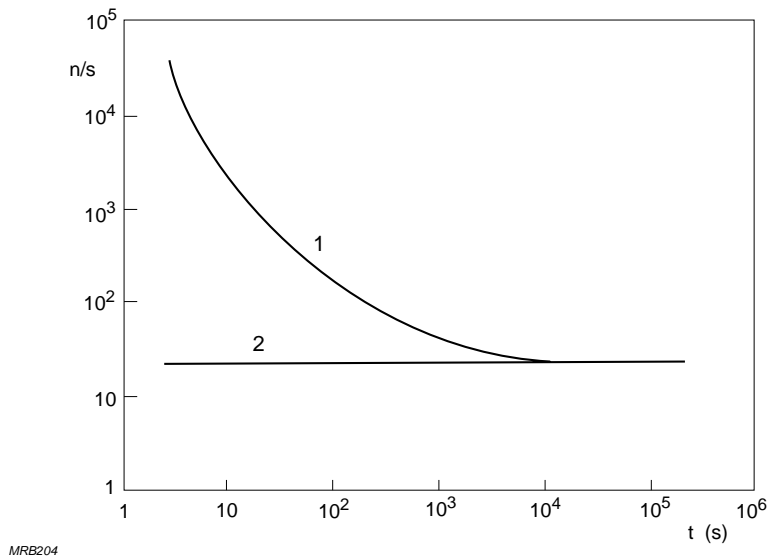


Fig.3.6 Dark-current behaviour following application of high voltage in 1) negative, 2) positive polarity. Vertical scale, number of dark pulses per second

### 3.2 Statistical nature of noise

It is important to recognize the irreducible nature of noise, which always accompanies the signals to be measured and cannot be cancelled or compensated. All the causes of noise encountered in photomultipliers have a common physical origin, namely the spontaneous fluctuation of currents and voltages due mainly to the discontinuous nature of radiation, electricity and matter. Noise is, therefore, closely related to the

statistical nature of photoemission and secondary emission and is inherent in the signal. Consider the following example.

A photomultiplier with a cathode sensitivity  $S_k = 10 \text{ mA/W}$  and operated at a gain  $G = 10^6$  is exposed to a continuous flux  $\Phi_e = 10^{-9} \text{ W}$ . The resulting anode voltage across a load resistance  $R_L = 5 \text{ k}\Omega$  is  $V_a = \Phi_e S_k G R_L = 50 \text{ mV}$ . However, when this is applied to an oscilloscope with a stray capacitance of  $50 \text{ pF}$  (equivalent noise band  $B_N = 1/4R_L C = 1 \text{ MHz}$ ) a peak-to-peak fluctuation of about  $\pm 20 \text{ mV}$  is observed, corresponding to an anode current fluctuation of  $\pm 4 \text{ }\mu\text{A}$ . That this fluctuation is noise inherent in the signal is evidenced by the fact that it disappears completely when the incident flux is removed. In this example, the fluctuation is relatively large because the number of photoelectrons emitted in a single period, corresponding to the reciprocal of the noise band ( $1/B_N = 1 \text{ }\mu\text{s}$ ), is small and fluctuates considerably from one period to the next.

If the incident flux is not continuous but pulsed, the resulting anode current fluctuates from pulse to pulse. The amplitude of the fluctuation determines the energy resolution of the photomultiplier; it is of the same statistical nature as the noise and yields to the same analytical procedures.

### 3.2.1 Photon noise

Photon emission is a random process, the number of photons emitted during like intervals being subject to a statistical distribution. To begin with we shall assume that fluctuations in the number of photons striking the cathode and the number of photoelectrons emitted both follow a *Poisson distribution*.

Consider a photocathode constantly illuminated by a source (e.g. a tungsten filament lamp) from which photons are emitted independently of each other. Assume that  $N_p$  photons are received by the photocathode during a fairly long period  $T$  (Fig.3.7). We can divide this period into a large number of intervals  $\tau$ . A photon emitted during the period  $T$  has a probability  $p = \tau/T$  of being received during an interval  $\tau$  and a probability  $(1 - p)$  of being received during the complementary interval  $(T - \tau)$ .

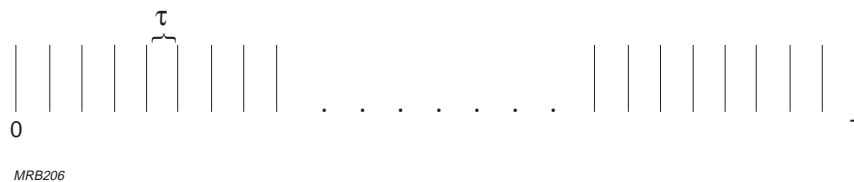


Fig.3.7 The probability of a photon arriving during the interval  $\tau$  is  $p = \tau/T$

All photons emitted during the period  $T$  have the same probability  $p$  of being received during an interval  $\tau$ . If the number of photons reaching the cathode during the period  $T$  is  $N_p$ , and the number during the interval  $\tau$  is  $n_{p,\tau}$ , then the number during the complementary interval  $(T - \tau)$  is  $(N_p - n_{p,\tau})$ . Thus, the possible number of combinations of  $N_p$  photons taken  $n_{p,\tau}$  at a time during the period  $T$  is

$$\binom{N_p}{n_{p,\tau}} = \frac{N_p!}{n_{p,\tau}!(N_p - n_{p,\tau})!}$$

and the probability  $P(n_{p,\tau})$  of obtaining  $n_{p,\tau}$  photons during the interval  $\tau$  is

$$P(n_{p,\tau}) = \binom{N_p}{n_{p,\tau}} \left(\frac{\tau}{T}\right)^{n_{p,\tau}} \left(1 - \frac{\tau}{T}\right)^{N_p - n_{p,\tau}} \quad (3.2)$$

This is the *binomial distribution*, with mean value

$$\bar{n}_{p,\tau} = N_p \frac{\tau}{T} = \bar{n}_p \tau$$

and standard deviation

$$\sigma = \sqrt{N_p \frac{\tau}{T} \left(1 - \frac{\tau}{T}\right)} = \sqrt{\bar{n}_p \tau \left(1 - \frac{\tau}{T}\right)}$$

where  $\bar{n}_p = N_p/T$  is the average number of photons received per unit time.

If  $T$  is taken fairly large or, which amounts to the same, if the probability  $p = \tau/T$  is very small, the binomial distribution tends towards the *Poisson distribution*:

$$P(n_{p,\tau}) = \frac{(\bar{n}_{p,\tau})^{n_{p,\tau}} \exp(-\bar{n}_{p,\tau})}{n_{p,\tau}!} \quad (3.3)$$

In this case, the mean value and the standard deviation are, respectively

$$\begin{aligned} \bar{n}_{p,\tau} &= \bar{n}_p \tau \\ \sigma_{n_{p,\tau}} &= \sqrt{\bar{n}_{p,\tau}} = \sqrt{\bar{n}_p \tau} \end{aligned} \quad (3.4)$$

Hence, the relative variance is

$$V_{n_{p,\tau}} = \frac{\sigma_{n_{p,\tau}}^2}{\bar{n}_{p,\tau}^2} = \frac{1}{\bar{n}_{p,\tau}} = \frac{1}{\bar{n}_p \tau} \quad (3.5)$$

from which it is evident that the larger the mean number of photons received during the interval  $\tau$ , the smaller are the fluctuations in the number.

### 3.2.2 Cathode current fluctuations

Photoemission is a random process which can usually be treated on its own. Each photon that strikes the cathode has a probability  $\rho$  (quantum efficiency) of liberating an electron and a probability  $(1 - \rho)$  of not liberating one. When the randomness of photon arrival is also to be taken into account, the mean value  $\bar{n}_{k,\tau}$  and standard deviation  $\sigma$  of the number of photoelectrons emitted during an interval  $\tau$  are, respectively

$$\begin{aligned} \bar{n}_{k,\tau} &= \bar{n}_p \rho \tau \quad \text{and} \\ \sigma_{n_{k,\tau}} &= \sqrt{\bar{n}_p \rho \tau} \end{aligned} \quad (3.6)$$

Hence the relative variance is

$$V_{n_{k,\tau}} = \frac{\sigma_{n_{k,\tau}}^2}{\bar{n}_{k,\tau}^2} = \frac{1}{\bar{n}_{k,\tau}} = \frac{1}{\bar{n}_p \rho \tau} \quad (3.7)$$

For the interval  $\tau$  the value of the cathode current  $I_{k,\tau}$  is given by

$$I_{k,\tau} = \frac{e n_{k,\tau}}{\tau}$$

where  $e$  is the electron charge.  $I_{k,\tau}$  differs from the mean current over a large number of intervals,  $I_k$ , by an amount

$$i_{k,\tau} = I_{k,\tau} - I_k = \frac{e}{\tau} (n_{k,\tau} - \bar{n}_{k,\tau}) \quad (3.8)$$

the mean square value of which is

$$\overline{i_{k,\tau}^2} = \frac{e^2}{\tau^2} \sigma_{n_{k,\tau}}^2 = \frac{e^2 \bar{n}_p \rho}{\tau} = \frac{e I_k}{\tau} \quad (3.9)$$

### 3.2.3 Noise spectrum

When the photocathode is illuminated by a constant flux, the photocurrent  $I_k(t)$  consists of a constant component  $I_k$  and a fluctuating component  $i_k(t)$ :

$$i_k(t) = I_k(t) - I_k$$

Here,  $i_k(t)$  is a true random quantity whose mean value  $\bar{i}_k(t)$  over a long period  $T$  is zero. However, there may be a certain correlation between values of  $i_k(t)$  measured at different times; this is expressed by the *autocorrelation function*:

$$\gamma(s) = \overline{i_k(t) \cdot i_k(t + s)} \quad (3.10)$$

For  $s = 0$ , the autocorrelation function assumes a maximum equal to the mean square value  $\overline{i_k^2(t)}$ . As  $s$  increases,  $\gamma(s)$  decreases and tends towards zero. Thus, we can characterize  $i_k(t)$  by a time constant  $\tau_0$  such that  $\gamma(s)$  becomes less than a specified very low value ( $\gamma(s) \leq \epsilon$ ) for  $|s| \gg \tau_0$ . If  $\tau_0$  is very small compared with the observation time of the signal  $i_k(t)$ , which it usually is in practice, the correlation can be disregarded.

We can express the autocorrelation function  $\gamma(s)$  another way by using the Fourier transform

$$\gamma(s) = \int_0^{\infty} w(f) \cos(2\pi fs) df \quad (3.11)$$

where  $w(f)$  represents the spectral density or *noise spectrum* of  $i_k(t)$ . The inverse Fourier transform expresses the noise spectrum as a function of  $\gamma(s)$ :

$$w(f) = 4 \int_0^{\infty} \overline{i_k(t) \cdot i_k(t + s)} \cos(2\pi fs) ds \quad (3.12)$$

This is the Wiener-Khintchine theorem which shows that the spectral density is independent of the frequency as long as  $2\pi f\tau_0 \ll 1$ .

If we set  $s$  equal to zero in Eq.3.10 and 3.11, we obtain

$$\gamma(0) = \overline{i_k^2(t)} = \int_0^{\infty} w(f) df \quad (3.13)$$

which relates the spectral density to the mean square value of  $i_k(t)$ . The term  $\overline{i_k^2(t)}$  represents the total noise power throughout the frequency spectrum, as a function of the parameters that characterize the random nature of the photon emission and the photon-electron conversion.

Consider the mean value of the fluctuating component  $i_k(t)$  of the photocurrent over an interval  $\tau$  that is very small compared with the observation time:

$$i_{k,\tau} = \frac{1}{\tau} \int_t^{t+\tau} i_k(t) dt$$

The quantity  $i_{k,\tau}$  fluctuates randomly from one interval to another; its mean square value

$$\overline{i_{k,\tau}^2} = \frac{1}{\tau^2} \int_0^\tau \int_0^\tau i_k(t) i_k(t') dt dt'$$

is independent of time because of the stationary nature of the random variable  $i_k(t)$ . However, if  $\tau \gg \tau_0$ ,

$$\overline{i_{k,\tau}^2} = \frac{w(f)}{2\tau} \quad (3.14)$$

so, by substitution from Eq.3.9,

$$w(f) = 2eI_k \quad (3.15)$$

which shows that, in the frequency range where  $\tau \gg \tau_0$ , the spectral density  $w(f)$  is constant.

Finally, by combining Eq.3.13 and 3.15 we can write:

$$\overline{i_k^2}(t) = 2eI_k \int_0^\infty df$$

or, for a frequency interval  $\Delta f$ ,

$$\overline{i_k^2}(t) = 2eI_k \Delta f \quad (3.16)$$

which is the well known *Schottky* formula. Dividing by  $I_k^2$  and substituting from Eq.3.9, gives

$$\frac{\overline{i_k^2}(t)}{I_k^2} = \frac{2e\Delta f}{I_k} = \frac{2\Delta f}{\bar{n}_p \rho} \quad (3.17)$$

the square root of which is the reciprocal of the signal-to-noise ratio:

$$\frac{N}{S} = \sqrt{\frac{2\Delta f}{\bar{n}_p \rho}} \quad (3.18a)$$

So the signal-to-noise ratio due to cathode current fluctuation under conditions of constant illumination, is

$$\frac{S}{N} = \sqrt{\frac{\bar{n}_p \rho}{2\Delta f}} \quad (3.18b)$$

in the frequency interval  $\Delta f$ .

### 3.2.4 Noise in scintillation detectors

So far we have considered only the fluctuations of a continuous photocurrent due to constant illumination of the cathode. However, we can extend the same reasoning to the photocurrent of a scintillation detector, even though the scintillation photon pulses decay exponentially, provided we choose sampling intervals long enough to include effectively the whole of a scintillation. As a first approximation we can assume that the number of photons per scintillation,  $n_{p,s}$ , follows a Poisson distribution; if  $n_{p,s}$  is large, the Poisson distribution tends towards a gaussian distribution. The number of photoelectrons per scintillation,  $n_{k,s}$ , then also follows a gaussian distribution, with relative variance

$$v_{n_{k,s}} = \frac{\sigma_{n_{k,s}}^2}{\bar{n}_{k,s}^2} = \frac{1}{\bar{n}_{k,s}} \quad (3.19)$$

The probability distribution of the number of photoelectrons is usually determined on the basis of an anode pulse histogram generated by a multichannel pulse-height analyser. When the scintillations are due to monoenergetic radiation (e.g. X-or  $\gamma$ -rays), the histogram has a more or less well-defined peak corresponding to photoelectric absorption of the radiation in the scintillator. If the FWHM of the peak corresponds to  $\Delta n_{k,s}$  electrons emitted by the cathode, the energy resolution of the photomultiplier-scintillator combination is

$$R_e = \frac{\Delta n_{k,s}}{\bar{n}_{k,s}}$$

which, for a gaussian distribution, reduces to

$$R_e = 2.36\sqrt{v_{n_{k,s}}}$$

or, from Eq.3.19,

$$R_e = \frac{2.36}{\sqrt{\bar{n}_{k,s}}} \quad (3.20)$$

Comparison of Eq.3.20 and 3.18 illustrates the close relation between energy resolution and signal-to-noise ratio.

### 3.2.5 Noise contribution of the electron multiplier

To take account of fluctuations in the secondary emission of the dynodes, a more extended treatment is required. Fluctuations in electron multiplication have been treated statistically by Lombard and Martin, using the method of generating functions; here, we merely summarize the main results.

First, assume that the random processes at all stages of the electron multiplier obey a Poisson distribution and occur independently of each other. The number of electrons reaching the anode during an interval  $\tau$  is

$$n_{a,\tau} = n_{k,\tau} G = n_{p,\tau} \rho G \quad (3.21)$$

where  $G$  is the photomultiplier gain. The relative variance of  $n_{a,\tau}$  is

$$v_{n_{a,\tau}} = \frac{\sigma_{n_{a,\tau}}^2}{\bar{n}_{a,\tau}^2} = \frac{1}{\bar{n}_p \rho \tau} (1 + v_G) \quad (3.22)$$

where  $v_G$  is the relative variance of the gain. It has been shown that when all electron-multiplier stages except the first have the same gain  $g$ ,

$$v_G = v_\eta + \frac{1}{\eta} \cdot \frac{1}{g_1} \cdot \frac{g}{g-1} \quad (3.23)$$

where  $g_1$  is the (usually higher) gain of the first stage, and  $v_\eta$  is the relative variance of the collection efficiency  $\eta$  of the input optics. In the ideal case, when  $\eta$  is independent of the point on the photocathode from which the electrons originate,

$$v_\eta = \frac{1 - \eta}{\eta} \quad (3.24)$$

e.g. for  $\eta = 0.95$ ,  $v_\eta \approx 0.05$ .

If we introduce the fluctuating component  $i_a(t)$  of the anode current,

$$i_a(t) = I_a(t) - I_a = i_k(t) G$$

Eq.3.17 and 3.20 can be replaced by

$$\frac{\overline{i_a^2(t)}}{I_a^2} = \frac{2\Delta f}{\bar{n}_p \rho} (1 + v_G) = \frac{2e\Delta f}{I_k} (1 + v_G) \quad \text{and} \quad (3.25)$$

and

$$R_e = 2.36 \sqrt{\frac{1 + v_G}{\bar{n}_{k,s}}} \quad (3.26)$$

The Poisson distribution assumption for secondary emission is only a rough approximation. The single-electron spectrum, which reveals the probability distribution of the electron multiplier gain, provides an accurate means to test it experimentally.

Equation 3.23 can be restated in the form

$$v_G = v_\eta + \frac{v_M}{\eta} \quad (3.27)$$

where

$$v_M = \frac{1}{g_1} \cdot \frac{g}{g - 1} \quad (3.28)$$

is the relative variance of the electron multiplier gain. This can be calculated from the single-electron spectrum obtained as follows.

The cathode is illuminated by a constant flux sufficient to cause the emission of fewer than  $10^4$  electrons per second, so that the mean interval between successive electrons is at least 100  $\mu$ s. The resulting anode charges are then integrated with a time constant of less than 1  $\mu$ s so that each voltage pulse has a very low probability (< 1%) of being due to the emission of more than one electron at the cathode. The resulting anode pulse histogram obtained from a multichannel analyser constitutes the single-electron spectrum.

Figures 2.4 and 3.8 show examples of single-electron spectra obtained in this way from photomultipliers with focusing and with venetian-blind dynodes. In neither case is the Poisson-distribution assumption confirmed: the variance is larger than that given by Eq.3.28, the discrepancy being greater for venetian-blind than for focusing dynodes. Anything that interferes with the input system focusing or impairs the collection efficiency increases the variance.

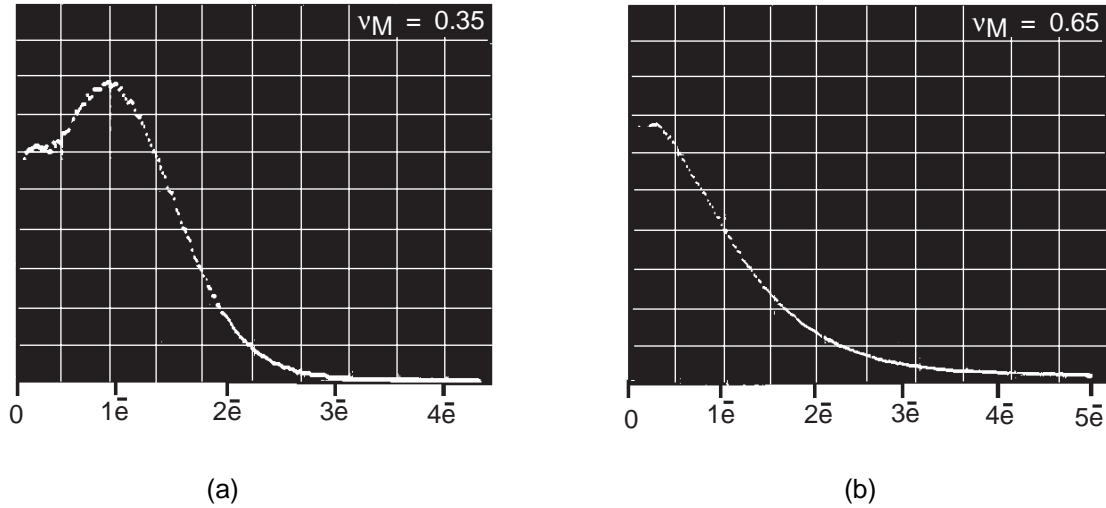


Fig.3.8 Single-electron spectra of photomultipliers with CuBe dynodes a) linear-focusing, b) venetian-blind. Vertical axes, pulse frequency (arbitrary scale; horizontal axes, anode pulse amplitude referred to number of electrons per pulse at the cathode

Considering that the relative variance  $v_G$  only appears as a corrective factor in Eq.3.25 and 3.26, it is simpler and sufficient to use Eq.3.27 and to consider  $v_\eta$  as an experimental factor. For tubes with focusing dynodes,  $v_\eta$  is between 0.1 and 0.2, depending on structural details and the voltages used. For venetian-blind dynode structures,  $v_\eta$  is between 0.2 and 0.4. At very low voltage (for example, 100 V between cathode and first dynode),  $v_\eta$  may be as high as 0.5.

Equation 3.28 has the merit of highlighting the predominant effect of the first-stage gain  $g_1$ . For example, if  $g_1 = 7$ ,  $g = 4$ , and  $v_\eta = 0.1$ ,  $v_G$  can be about 0.3; whereas if  $g_1 = g = 3$ , and  $v_\eta = 0.4$ ,  $v_G$  can be close to unity.

### 3.2.6 Johnson noise

Equation 3.25 can be rewritten as follows to give the reciprocal of the signal-to-noise ratio at the anode

$$\frac{N}{S} = \sqrt{\frac{\overline{i_a^2}}{I_a^2}} = \sqrt{\frac{2e\Delta f (1 + v_G)}{I_k}} = \sqrt{\frac{2e\Delta f (1 + v_G)}{\Phi S_k}} \quad (3.29)$$

where  $\Phi$  is the incident flux and  $S_K$  the cathode sensitivity. *Comparison of this with Eqs 3.17 and 3.18 illustrate one of the fundamental advantages of amplification by secondary emission; the signal-to-noise ratio is only slightly degraded (20% in the worst case) and, to a first approximation, is nearly independent of the gain used.* Hence, there is no objection to using the maximum gain, provided the mean anode current stays within the permissible limits and no feedback phenomena interfere with the operation (§5.5.2).

In any case, there is a minimum gain for which the signal noise (or shot noise) becomes predominant compared with the Johnson noise in the load resistance  $R_L$ . (For simplicity, intrinsic amplifier noise is here disregarded). The RMS value of the signal noise is given by

$$R_L \sqrt{i_a^2} = GR_L \sqrt{2e\Delta f (1 + v_G) I_k} \quad (3.30)$$

and the RMS value of Johnson noise by

$$\sqrt{4kTR_L\Delta f} \quad (3.31)$$

from which it is possible to calculate that the minimum gain for which the Johnson noise is negligible compared with the signal noise,

$$G \gg \sqrt{\frac{2kT}{eR_L I_k (1 + v_G)}} \quad (3.32)$$

or, with  $T = 300 \text{ K}$ ,  $k = 1.38 \times 10^{-23} \text{ J/K}$ ,  $v_G = 0.5$

$$G^2 \gg \frac{3.5 \times 10^{-2} (\text{V})}{R_L (\Omega) I_k (\text{A})}$$

An approximation giving a reasonable margin of safety is

$$G_{\min}^2 = \frac{1 (\text{V})}{R_L (\Omega) I_k (\text{A})} \quad \text{or} \quad G_{\min} = \frac{1 (\text{V})}{R_L (\Omega) I_a (\text{A})} \quad (3.33)$$

where the mean anode current  $I_a = GI_k$

### 3.2.7 Scintillation detection

*Pulse mode.* This is the mode used in nuclear spectrometry. Equation 3.26 shows that if the number of light photons per scintillation is proportional to the energy  $E_{ph}$  of the X- or  $\gamma$ -photons absorbed in the scintillator, the energy resolution should vary inversely as  $\sqrt{E_{ph}}$ . However, this is not observed experimentally, especially at high energy levels. When the  $\gamma$ -radiation of  $^{137}\text{Cs}$  (662 keV) is absorbed in a NaI(Tl) scintillator for example, the number of photons emitted should give a resolution of about 5%; however, the value observed experimentally is closer to 7%. Reasons for the discrepancy are:

- scintillation efficiency is not uniform throughout the bulk of the scintillator;
- cathode sensitivity is not uniform – scintillations from different parts of the scintillator give rise to different numbers of electrons;
- variations in the energy conversion process in the scintillator.

Faulty optical coupling, incomplete collection at the first dynode, or anything tending to impair cathode uniformity also impairs the energy resolution.

A theoretical analysis which has served as the basis for all subsequent statistical treatments of energy spectrometry has shown that the energy resolution can be expressed by the general equation

$$R_e = 2.36 \sqrt{\left( v_{n\ p,s} + \frac{1 - \rho + v_G}{\bar{n}_{p,s} \rho} \right)} \quad (3.34)$$

where  $\rho$  is the photocathode quantum efficiency,  $v_G$  the relative variance of the photomultiplier gain (Eq.3.23 or 3.27) and  $v_{n\ p,s}$  the relative variance of the photon distribution, which must be determined empirically.

Letting  $k = E_{ph}/\bar{n}_{p,s}$  represent the ratio of the initial energy of the X- or  $\gamma$ -photons completely absorbed in the scintillator to the mean number of photons received by the photocathode, Eq.3.34 can be rewritten in the form

$$R_e^2 = \alpha + \frac{\beta}{E_{ph}} \quad (3.35)$$

where

$$\alpha = 2.36^2 v_{n\ p,s}$$

and

$$\beta = 2.36^2 (1 - \rho + v_G) \frac{k}{\rho}$$

In Fig.3.9, a straight line corresponding to Eq.3.35 is superimposed on values obtained by measurement. At energies below about 300 keV Eq.3.35 is in good agreement. From the intersection of the line with the ordinate it is possible to determine  $\alpha$  and  $v_{n\ p,s}$  empirically. At higher energies the resolution is better than predicted by Eq.3.35, as shown by the measured values being below the straight line. Various explanations for this have been proposed.

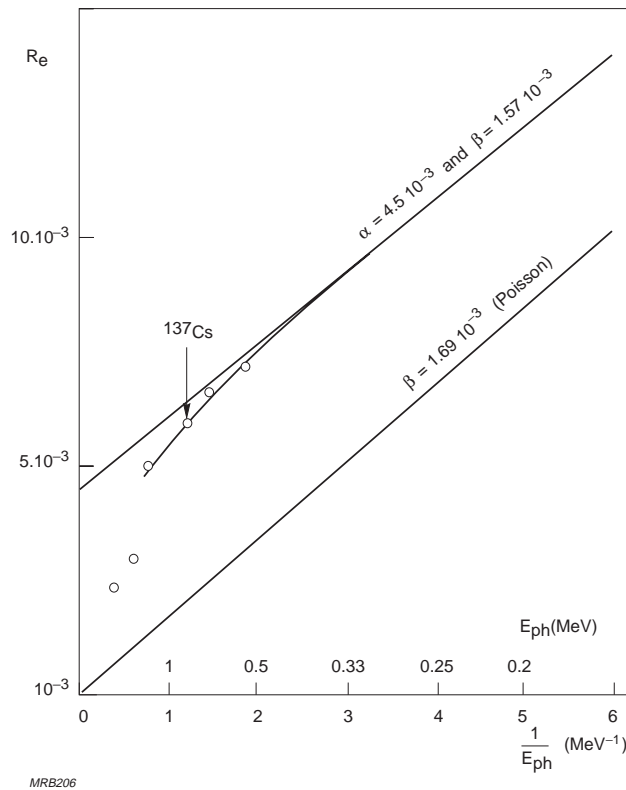


Fig.3.9 Energy resolution as a function of the X or  $\gamma$  photon energy  $E$  absorbed in the scintillator

The lower line in Fig.3.9 is based on an assumed Poisson distribution,  $v_{n p,s} = 1/\bar{n}_{p,s}$ , for which Eq.3.35 simplifies to

$$R_e^2 = \frac{\beta'}{E_{ph}}$$

where  $\beta' = 2.36^2 (1 + v_G) k/\rho$ . This is identical to Eq.3.26 and represents a limiting case for energy resolution; the slope of the line depends on the quantum efficiency and the variances of the gain.

*Continuous mode.* In some applications, scintillation detectors are used in a continuous mode. In scanning electron microscopy, for example, electrons reflected from a specimen are accelerated onto a scintillator and the resulting output of a photomultiplier provides the video signal for a television monitor. Continuous thickness measurements of sheet metal, paper, etc. by the absorption of  $\beta$ - or  $\gamma$ -radiation are also based on this mode.

The quantity to be measured is the arrival rate of the quanta (X-,  $\gamma$ -photons,  $\alpha$ -,  $\beta$ -particles, etc.). However, because some give rise to no scintillation, there is an

uncertainty in the number of quanta,  $n_q$ , which depends on the probability  $p$  of their interaction with the scintillator. Thus, if  $Q$  is the ratio of the number of electrons received at the anode,  $n_a$ , to the number of interactions in the scintillator per unit of time,

$$Q = \frac{n_a}{n_q p} \quad \text{and}$$

$$n_a = n_q p Q \quad (3.36)$$

which is equivalent to Eq.3.21, so the same analysis applies. Replacing the number of photons  $n_{p,\tau}$ , the quantum efficiency  $\rho$  and the gain  $G$  by the  $n_q$ ,  $p$  and  $Q$  respectively, we can write Eq 3.17 in the form

$$\frac{\overline{i_k^2(t)}}{I_k^2} = \frac{2\Delta f}{\overline{n_q p}} \quad (3.37)$$

This allows only for fluctuations in the number of interactions in the scintillator; however, the number of photons created per interaction, the number of photoelectrons emitted, and the number of secondary electrons are also subject to fluctuation, independently of each other and of the number of scintillator interactions. Fortunately, the total of these fluctuations can be evaluated on the basis of the anode pulse amplitude distribution corresponding to the *single-quantum spectrum* (SQS). This can be determined with a multichannel analyser by irradiating the scintillator with quanta of the type in question (X- or  $\gamma$ -photons,  $\alpha$ -,  $\beta$ -particles, etc.). The spectrum is characterized by a relative variance  $v_Q$ . With an NaI(Tl) scintillator, for example, this ranges from 0.002 for the  $\gamma$ -radiation of  $^{57}\text{Co}$  ( $E_\gamma = 122$  keV) to 0.450 for the  $\gamma$ -radiation of  $^{137}\text{Cs}$  ( $E_\gamma = 662$  keV). Some spectra with an exponential shape or with widely separated peaks (§A.3) can have a variance close to unity. By analogy with Eq.3.25,  $v_G$  can be replaced by  $v_Q$  and Eq.3.37 rewritten in the form

$$\frac{\overline{i_a^2(t)}}{I_a(t)^2} = \frac{2\Delta f}{\overline{n_q p}} (1 + v_Q) \quad (3.38)$$

$v_Q$ , like  $v_G$ , is a corrective term that lowers the S/N ratio by a factor  $1/(1+v_Q)^{1/2}$ , which is usually between 0.7 and 0.9; the number of interactions in the scintillator remains the predominant factor. Table 3.1 compares the parameters used in the pulse-mode and analogue-mode analysis and illustrates their close parallelism.

Table 3.1

Statistical parameters in the detection of continuous light and scintillation pulses.

continuous light	scintillation pulses
<div style="text-align: center;"> <div style="border: 1px solid black; padding: 5px; width: fit-content; margin: 0 auto;">photon flux</div> <p>⇓</p> <p><i>photon noise</i></p> <p>relative variance, <math>\frac{1}{\bar{n}_p}</math></p> </div>	<div style="text-align: center;"> <div style="border: 1px solid black; padding: 5px; width: fit-content; margin: 0 auto;">X, <math>\gamma</math>, <math>\alpha</math>, <math>\beta</math> quanta, etc.</div> <p>⇓</p> <p><i>quantum noise</i></p> <p>relative variance, <math>\frac{1}{\bar{n}_q}</math></p> </div>
<div style="text-align: center;"> <div style="border: 1px solid black; padding: 5px; width: fit-content; margin: 0 auto;">photoemission quantum efficiency, <math>\rho</math></div> <p>⇓</p> <p><i>random number of photoelectrons</i></p> <p>relative variance, <math>\frac{1}{\bar{n}_p \rho}</math></p> </div>	<div style="text-align: center;"> <div style="border: 1px solid black; padding: 5px; width: fit-content; margin: 0 auto;">scintillator interactions interaction probability, <math>p</math></div> <p>⇓</p> <p><i>random number of scintillations</i></p> <p>relative variance, <math>\frac{1}{\bar{n}_q p}</math></p> </div>
<div style="text-align: center;"> <div style="border: 1px solid black; padding: 5px; width: fit-content; margin: 0 auto;">multiplication by secondary emission</div> <p>⇓</p> <p><i>single-electron spectrum (SES)</i></p> <p>relative variance, <math>v_M \rightarrow v_G</math></p> </div>	<div style="text-align: center;"> <div style="border: 1px solid black; padding: 5px; width: fit-content; margin: 0 auto;">photon-current conversion</div> <p>⇓</p> <p><i>single-quantum spectrum (SQS)</i></p> <p>relative variance, <math>v_Q</math></p> </div>
<div style="text-align: center;"> <p><i>noise-to-signal ratio</i></p> <math display="block">\frac{N}{S} = \sqrt{\frac{2\Delta f(1 + v_G)}{\bar{n}_p \rho}} \quad (\text{Eq.3.25})</math> </div>	<div style="text-align: center;"> <p><i>noise-to-signal ratio</i></p> <math display="block">\frac{N}{S} = \sqrt{\frac{2\Delta f(1 + v_Q)}{\bar{n}_q p}} \quad (\text{Eq.3.38})</math> </div>

### 3.3 Equivalent noise input and minimum discernible signal

Because the noise sources dealt with so far cause uncertainty in the detection of small signals or inaccuracy in their measurement, we have pursued an analysis that emphasizes the relation between noise and energy resolution and leads to a mathematical expression for signal-to-noise ratio. Now we shall give a more general definition of signal-to-noise ratio and introduce the new quantities, *noise equivalent power* and *equivalent noise input*. These can be measured experimentally and used for determining the *minimum discernible signal*. In practice, however, the minimum discernible signal also depends on the method of detection, the observer, and the probability that can be accepted of obtaining a spurious signal.

#### 3.3.1 Definitions

Several definitions relating to maximum sensitivity are sanctioned by usage or recommended by the IEC. However there are still no full and precise standards on the subject. Here we shall give the most useful definitions, together with the abbreviations under which they are often known.

*Equivalent anode dark current input*, EADCI, of an individual photomultiplier is the flux that must be applied to the photocathode to produce an anode current equal to the dark current  $I_{ao}$ . Hence, it is the ratio of the anode dark current to the anode sensitivity

$$\text{EADCI} = \frac{I_{ao}}{S_a} \quad (3.39)$$

expressed in watts or lumens, depending on the unit of  $S_a$ . It varies greatly with the experimental conditions (temperature, humidity, stabilizing time), and is of practical interest only when the tube is operating continuously.

*Signal-to-noise ratio*, S/N, defined at the system output is the ratio between the RMS values of the output signal and the overall noise (signal noise plus dark current noise) within the system bandwidth.

*Noise equivalent power*, NEP, (symbol  $P_N$ ) is the incident flux that produces an RMS output signal equal to the RMS noise measured at the output under specific operating conditions. It may be expressed in watts or lumens depending on the nature of the application and the incident flux, and is significant only in relation to the specified set of operating conditions; (for instance: incident flux spectrum, modulation frequency, measuring equipment bandwidth, illuminated cathode area, operating temperature). The lower the noise equivalent power, the better the photomultiplier is able to detect low flux inputs.

Some publications specify  $P_N$  for a bandwidth of 1 Hz based on the assumption of constant spectral density throughout the frequency range concerned. It is then expressed in  $W/Hz^{1/2}$  or  $lm/Hz^{1/2}$ .

*Equivalent noise input*, ENI, (symbol  $E_N$ ) is the ratio of the noise equivalent power to the area of the cathode, assuming the whole cathode to be uniformly illuminated. It is expressed in  $W/m^2$  or  $lm/m^2$ . For a bandwidth of 1 Hz it is expressed in  $W/m^2 Hz^{1/2}$  or  $lm/m^2 Hz^{1/2}$ . Like noise equivalent power, a specified equivalent noise input is significant only in relation to a specified set of operating conditions.

*Detectivity*,  $D$ , is the reciprocal of the noise equivalent power:

$$D = \frac{1}{P_N} \quad (3.40)$$

It is expressed in  $W^{-1}$  or  $lm^{-1}$ .

### 3.3.2 Minimum value of noise equivalent power

The photomultiplier and its load resistance account for the greater contribution to the total noise measured, the electronics for a much smaller contribution. Two of the main sources of noise are:

- the shot noise associated with the photomultiplier signal current, Eq.3.30
- the Johnson noise due to the load resistance, Eq.3.31.

Both apply over a frequency interval of  $\Delta f$ . All the other causes of noise can be taken into account by assuming an additional random component of the anode current with a mean square value  $\overline{i_{a,n}^2}$  over the interval  $\Delta f$ . The signal-to-noise ratio of the photomultiplier is then

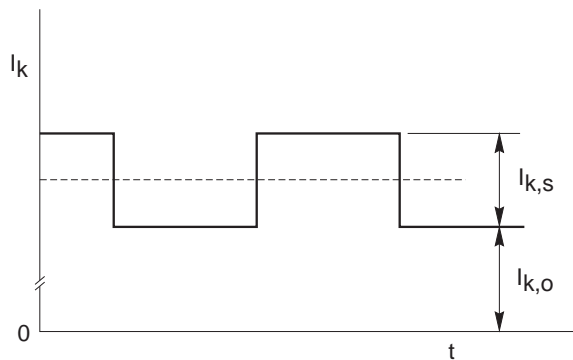
$$\frac{S}{N} = \frac{I_a}{\sqrt{\frac{4kT\Delta f}{R_L} + 2e G^2 I_k \Delta f (1 + v_G) + \overline{i_{a,n}^2}}} \quad (3.41)$$

The term  $\overline{i_{a,n}^2}$  mainly represents the noise associated with the different components of the dark current (thermionic noise, field emission noise, etc.) plus such additional noise as the input noise of the electronics. It does not necessarily obey the Schottky formula, nor should it be regarded as wideband white noise; it is sufficient to bear in mind that it applies to a frequency interval  $\Delta f$  equal to the energy bandwidth  $B_N$ , or *equivalent noise bandwidth*, of the measuring circuit.

It is more convenient to express the signal-to-noise ratio as a function of the cathode current; Eq.3.41 then becomes

$$\frac{S}{N} = \frac{I_k}{\sqrt{B_N \left( \frac{4kT}{G^2 R_L} + 2eaI_k + \frac{\overline{i_{k,n}^2}}{B_N} \right)}} \quad (3.42)$$

where  $a = 1 + v_G$  and  $\overline{i_{k,n}^2} = \overline{i_{a,n}^2} / G^2$  is the calculated additional anode noise referred to the cathode. In Eq.3.42 this term is referred to the unit of bandwidth ( $\overline{i_{k,n}^2} / B_N$ ).



MRB207

Fig.3.10 Cathode current when the input flux is chopped

Equation 3.42 shows that *the most effective way to improve the signal-to-noise ratio is to reduce the bandwidth  $B_N$  of the measuring circuit*, at least in the frequency range where the  $\overline{i_{k,n}^2} / B_N$  is still small. A light modulator combined with a very narrow band AC amplifier is often used for this (Fig.3.13) and has the advantage of automatically cancelling the DC component of the dark current, although the noise associated with the dark current is amplified normally. If the amplifier bandwidth is very narrow (a few hertz), only the fundamental component of the modulated signal is amplified.

If the light is modulated by a symmetrical square wave (Fig.3.10), the RMS value of the fundamental component of the cathode current due to the signal is

$$\frac{I_{k,s}}{\pi} \sqrt{2} \quad (3.43)$$

and the mean noise current associated with the signal and measured in the equivalent noise bandwidth  $B_N$  is

$$\overline{i_{k,s}^2} = \frac{2ea I_{k,s} B_N}{2}$$

Therefore, assuming that  $G^2RL$  is large enough to allow the Johnson noise to be neglected, the ratio of the RMS signal and noise currents is

$$\frac{S}{N} = \frac{I_{k,s}}{\pi} \sqrt{\frac{2}{\left( eaI_{k,s}B_N + \overline{i_{k,n}^2} \right)}} \quad (3.44)$$

The noise equivalent power,  $P_N$ , is found by setting the S/N ratio equal to unity:

$$P_N = \frac{I_{k,s}}{S_k} \text{ at } \frac{S}{N} = 1 \quad (3.45)$$

If the equivalent noise bandwidth  $B_N$  tends towards zero,

$$\lim_{B_N \rightarrow 0} \frac{P_N}{\sqrt{B_N}} = \frac{\pi}{S_k} \sqrt{\frac{\overline{i_{k,n}^2}}{2B_N}} \quad (3.46)$$

provided the spectral density  $\overline{i_{k,n}^2}/B_N$  tends towards a finite limit as  $B_N$  tends towards zero. This shows that  $P_N$  has significance only when the bandwidth is defined in which  $\overline{i_{k,n}^2}$  is specified (width and centre frequency). The value of  $\sqrt{\overline{i_{k,n}^2}/B_N}$  can be of the order of  $10^{-16}$  A/Hz<sup>1/2</sup> for a photomultiplier having a photoemission threshold in the visible spectrum ( $W_{ph} > 1.5$  eV).

A limiting case to consider is that in which the noise component  $\overline{i_{k,n}^2}$  represents only the noise power associated with the dark current, that is to say

$$\overline{i_{k,n}^2} = 2ea I_{ko} B_N \quad (3.47)$$

where  $I_{ko}$  is the equivalent dark current of the photocathode, corresponding to the anode dark current divided by the gain,  $I_{ko} = I_{ao}/G$ . Equation 3.47 represents a minimum value for the noise component  $\overline{i_{k,n}^2}$ , disregarding the DC component of the dark current (i.e. the leakage current, which is usually negligible) and the noise contribution of the measuring circuits. The minimum noise equivalent power  $P_N$  referred to the bandwidth is then

$$\lim_{B_N \rightarrow 0} \left( \frac{P_N}{\sqrt{B_N}} \right) = \frac{\pi}{S_k} \sqrt{eaI_{ko}} \quad (3.48)$$

### 3.3.3 Effect of bandwidth

Equation 3.48 is valid only when the bandwidth is very small (a few hertz); we shall now consider how the noise equivalent power varies as bandwidth increases.

Assume that the bandwidth of the amplifier in the measuring circuit is equivalent to that of an RC circuit, the DC component of the signal being blocked (Fig.3.13). When the incident flux is modulated by a symmetrical square wave (Fig.3.10), the RMS value of the periodic component of the cathode current due to the signal is

$$\sqrt{(I_k - I_{ko})^2} = m \frac{I_{k,s}}{2} \quad (3.49)$$

where the modulation coefficient  $m \leq 1$  and depends on the bandwidth and modulation frequency. If the bandwidth is taken as the 3 dB cut-off frequency of the RC circuit.

$$B_{3dB} = f_c = \frac{1}{2\pi RC}$$

and the modulation frequency  $f_m$  as 100 Hz, Fourier analysis shows that the value of  $m$  is

$$m = \frac{2}{\pi} \sqrt{2 \sum_{n=1}^{\infty} \frac{1}{(2n-1)^2} \cdot \frac{1}{1 + \left(\frac{100(2n-1)}{B_{3dB}}\right)^2}}$$

Figure 3.11 shows the variation of  $m$  as a function of  $B_{3dB}$ . The signal-to-noise ratio is thus

$$\frac{S}{N} = \frac{m I_{k,s}}{2 \sqrt{\left\{ e a I_{k,s} B_N + \overline{i_{k,n}^2} \right\}}} \quad (3.50)$$

and, from Eq.3.45, the noise equivalent power is

$$P_N = \frac{2eaB_N}{m^2 S_K} \left\{ 1 + \sqrt{1 + \frac{m^2 \overline{i_{k,n}^2}}{e^2 a^2 B_N^2}} \right\} \quad (3.51)$$

When the bandwidth is high (in practice,  $B_{3dB} > 10^3$  Hz),  $m$  tends towards unity and the expression for  $P_N/NB_N$  tends towards

$$\lim_{B_N \rightarrow \infty} \left( \frac{P_N}{\sqrt{B_N}} \right) = \frac{4ea}{S_k} \sqrt{B_N} \quad (3.52)$$

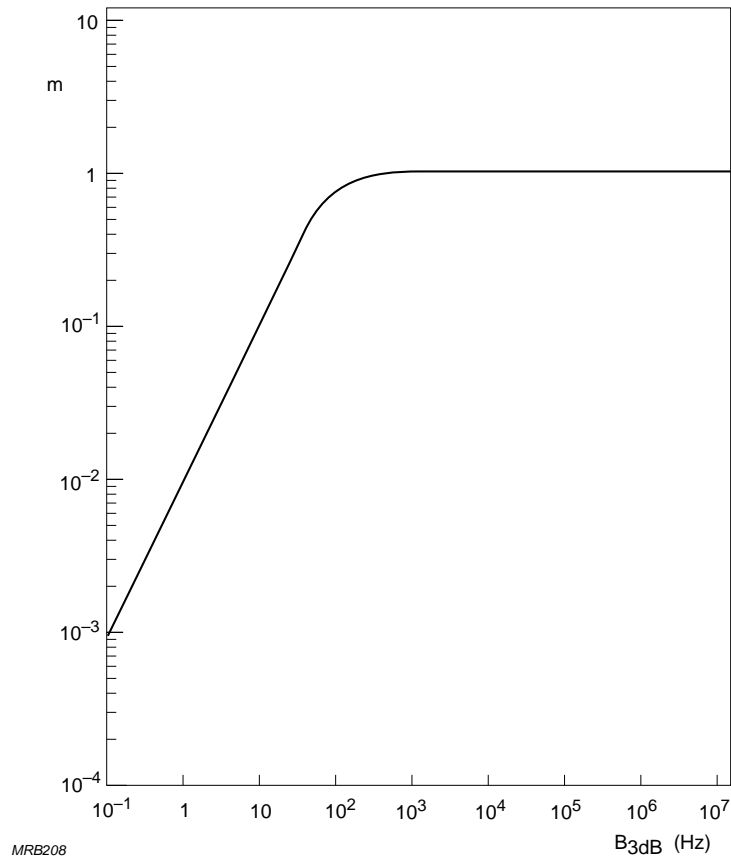


Fig.3.11 Modulation coefficient  $m$  as a function of the 3 dB bandwidth of the measuring circuit. ( $f_m = 100$  Hz)

Figure 3.12 shows the variation in the noise equivalent power  $P_N$  as a function of the energy bandwidth  $B_N$  for two values of  $i_{k,n}^2$ . The solid line on the left correspond to very low values of bandwidth ( $B_N < 10$  Hz) centred about the fundamental frequency of the modulated signal. This is where the smallest value of the noise equivalent power is obtained; the practical minimum is determined by the noise associated with the dark current, hence the interest in keeping the dark current as low as possible. The solid lines on the right correspond to high values of bandwidth ( $B_N > 10^3$  Hz, for a modulation frequency of 100 Hz). This is where the noise equivalent power  $P_N$  becomes proportional to the energy bandwidth of the measuring circuit.

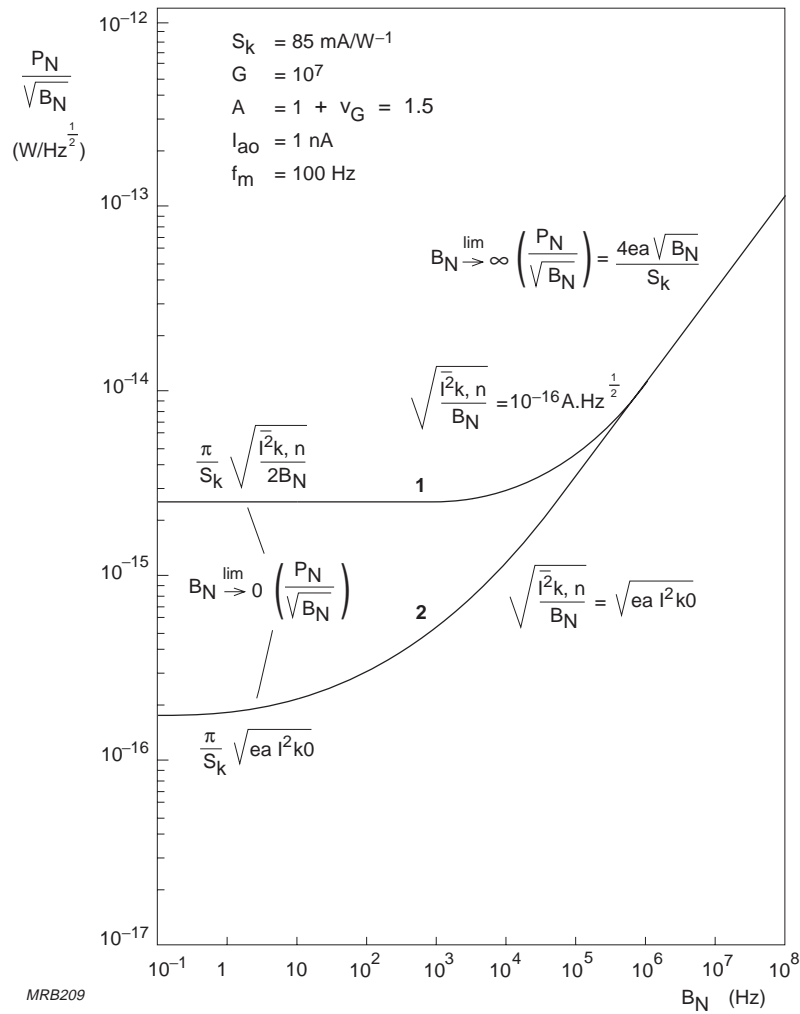


Fig.3.12 Noise equivalent power (flux as a function of the measuring circuit passband, for two value of additional noise: 1)  $10^{-16} \text{ A/Hz}^{1/2}$ , 2)  $7 \times 10^{-18} \text{ A/Hz}^{1/2}$

### 3.3.4 Measurement of noise equivalent power

Figure 3.13 shows the set-up used for determining the minimum value of the noise equivalent power. The incident flux is mechanically chopped to obtain a symmetrical square-wave voltage at the photomultiplier anode; the usual chopping frequency is 100 Hz. The photomultiplier signal is applied to a filter with a 3 dB bandwidth of 1000 Hz (the preceding amplifier blocks the DC component). A voltmeter measures the RMS value of the amplified voltage.

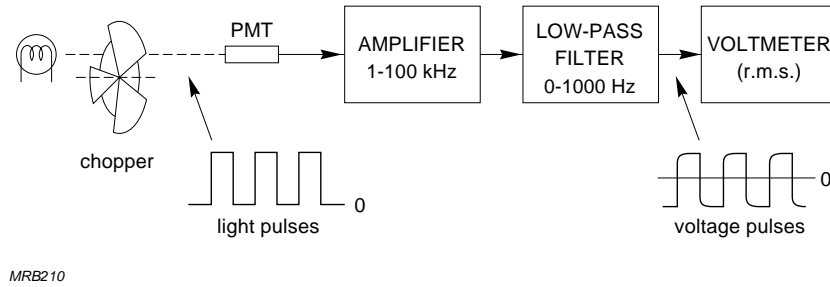


Fig.3.13 Set-up for measuring noise equivalent power

The minimum noise equivalent power is determined by measuring the signal-to-noise ratio. The effective bandwidth of the measuring set-up being 1000 Hz, the signal-to-noise ratio at a bandwidth of 1 Hz is obtained by calculation. Two measurements are carried out in succession:

- first, with no light, the RMS noise voltage  $V_N$  is measured for an energy bandwidth  $B_N = (\pi/2)1000$  Hz. Assuming the spectral density of the noise to be constant throughout the frequency range under consideration, the RMS noise voltage for a bandwidth of 1 Hz is then

$$V_N (1 \text{ Hz}) = \frac{V_N}{\sqrt{\frac{\pi}{2} 1000}} \quad \text{V/Hz}^{1/2} \quad (3.53)$$

- next, with chopped light, the RMS signal voltage  $V_S$  is measured for a 3 dB bandwidth of 1000 Hz. The RMS value calculated for a bandwidth of 1 Hz is the RMS value of the fundamental component of the modulated voltage. Thus, from Eq.3.43 and 3.49,

$$V_S (1 \text{ Hz}) = \frac{2V_s\sqrt{2}}{m\pi}$$

where  $m$  takes account of the finite bandwidth (Fig.3.11). For a bandwidth of 1000 Hz and a modulation frequency of 100 Hz,  $m = 0.968$ ; hence,

$$V_s (1 \text{ Hz}) = 0.930 V_s \quad (3.54)$$

Thus, from Eqs 3.53 and 3.54, for an energy bandwidth of 1 Hz,

$$\frac{V_S (1 \text{ Hz})}{V_N (1 \text{ Hz})} = 0.930 \frac{V_S}{V_N} \sqrt{1000 \frac{\pi}{2}}$$

Finally, the minimum noise equivalent power is given by

$$P_N = \Phi \frac{V_N (1 \text{ Hz})}{V_S (1 \text{ Hz})} \quad (3.55)$$

or

$$P_N = \frac{V_N \Phi}{0.930 V_S \sqrt{1000 \frac{\pi}{2}}} \quad (3.56)$$

expressed in  $\text{W/Hz}^{1/2}$  or in  $\text{lm/Hz}^{1/2}$  depending on the unit of incident flux,  $\Phi$ .

## APPENDIX 3

### A3.1 Practical scintillation spectra

*β-spectrum* The β-spectrum is intermediate between the uniform and the triangular distributions; its relative variance  $v$  is close to 0.4.

*γ-spectrum* consisting of a single gaussian peak ( $^{55}\text{Fe}$ ,  $^{57}\text{Co}$ ),  $R_e = 2.36\sqrt{v}$ .

$$^{55}\text{Fe}: E_\gamma = 5.9 \text{ keV}, R_e = 0.40, v = 2.9 \times 10^{-2}$$

$$^{57}\text{Co}: E_\gamma = 122 \text{ keV}, R_e = 0.10, v = 1.8 \times 10^{-3}$$

*γ-spectrum with Compton distribution* For a typical case,  $^{137}\text{Cs}$  ( $E_\gamma = 662 \text{ keV}$ ),  $v \approx 0.45$ .

*Complex spectrum with several peaks approximating delta functions* When the peaks are narrow and entirely separate  $v$  is between 0.5 and 1.

### A3.2 Noise equivalent bandwidth

Consider a linear transmission system having a transfer function  $G(f)$  for a signal of frequency  $f$  and unit amplitude. If a randomly varying signal  $i(t)$  – for example, the noise component of photomultiplier anode current – is applied to such a system, its response  $i_s(t)$  is given by

$$\overline{i_s^2(t)} = \int_0^\infty w(f) |G(f)|^2 df$$

where  $w(f)$  is the energy density spectrum of  $i(t)$ .

If  $w(f)$  can be assumed to be independent of frequency so that it can be replaced by a constant  $w_0$ , then the original transmission system can be replaced by a notional one which fulfils the following conditions:

- it transmits a constant power density equal to  $w_0 G_0^2$  throughout a frequency interval  $B_N = f_2 - f_1$ ;
- the total noise power it transmits throughout this interval is equal to that of the original system.

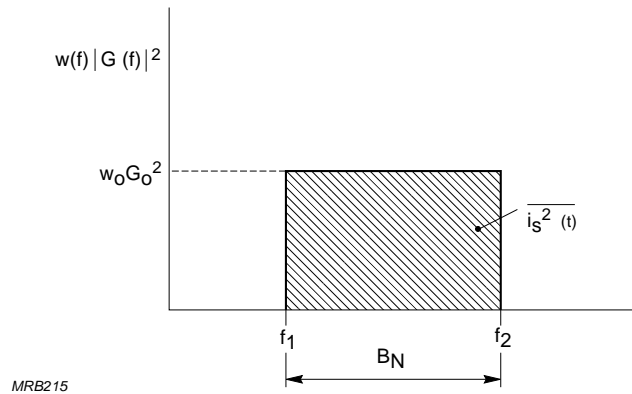


Fig.A3.1 Definition of noise pass-band  $B_N$ .

For such a system

$$w_0 G_0^2 B_N = w_0 \int_0^{\infty} |G(f)|^2 df$$

whence

$$B_N = \frac{1}{G_0^2} \int_0^{\infty} |G(f)|^2 df$$

where  $G_0$  may be either the maximum value of  $G(f)$  or its value at the centre frequency between  $f_1$  and  $f_2$ .

$B_N$  defines the energy bandwidth, or *noise equivalent bandwidth*, of the actual transmission system. The transfer function of such a system may take a variety of forms; a commonly encountered one is equivalent to that of an *RC* circuit,

$$|G(f)| = \frac{G_0}{1 + (2\pi f RC)^2}$$

for which  $B_{3dB} = 1/2\pi RC$  and the noise equivalent bandwidth is

$$B_N = \frac{1}{4RC} = \frac{\pi}{2} B_{3dB}$$

This treatment applies only to linear systems; non-linear systems require a more general interpretation of noise equivalent bandwidth.